Physics Letters A 380 (2016) 1658–1662

Contents lists available at ScienceDirect

Physics Letters A

www.elsevier.com/locate/pla

Low-temperature photoluminescence in self-assembled diphenylalanine microtubes

T. Nikitin [a], S. Kopyl [b], V.Ya. Shur [a], Y.V. Kopelevich [c,*], A.L. Kholkin [a,b,**]

[a] Institute of Natural Sciences, Ural Federal University, 620000 Ekaterinburg, Russia
[b] Physics Department & CICECO – Materials Institute of Aveiro, University of Aveiro, 3810-193 Aveiro, Portugal
[c] Instituto de Fisica, UNICAMP, Campinas, São Paulo 13083-859, Brazil

ARTICLE INFO

Article history:
Received 3 December 2015
Received in revised form 24 February 2016
Accepted 25 February 2016
Available online 2 March 2016
Communicated by L. Ghivelder

Keywords:
Diphenylalanine
Self-assembly
Photoluminescence
Exciton

ABSTRACT

Bioinspired self-assembled structures are increasingly important for a variety of applications ranging from drug delivery to electronic and energy harvesting devices. An important class of these structures is diphenylalanine microtubes which are potentially important for optical applications including light emitting diodes and optical biomarkers. In this work we present the data on their photoluminescent properties at low temperatures (down to 12 K) and discuss the origin of the emission in the near ultraviolet (UV) range seen earlier in a number of reports. UV luminescence increases with decreasing temperature and exhibits several equidistant lines that are assigned to zero-phonon exciton emission line and its phonon replicas. We infer that the exciton is localized on the defect sites and significant luminescence decay is due to thermal quenching arising from the carrier excitation from these defects and non-radiative recombination.

1. Introduction

Self-assembly of bioorganic nanomaterials has attracted significant interest due to various possibilities offered by their unique structure combined with design variability offered by non-covalent interactions in the structure [1–3]. Bioinspired amino acid- and peptide-based nanostructures are of special importance because they can be used in various applications ranging from biological scaffolds [4] and templates for nanowire fabrications [5] to light-emitting diodes (LED) [6] and gates for field-effect transistors [7]. The most studied self-organized peptide is diphenylalanine (FF) that combines fascinating physical properties with the ability to bind to several metals and other functional groups. It is derived from the core recognition motif of Alzheimer's disease β-amyloid polypeptide and thus is interesting from the biomedical point of view. It has been shown that FF-based materials are prone to self-assemble into tubular [8], spherical [9], rod-like [10], and fibrous structures [11] depending on the deposition method and solvent chemistry. Excellent mechanical [12], electrical [13], piezoelectric [14], optical [15], and electrochemical [16] properties have shown great potential of using FF-structures in nano- and microdevices. Strong blue and near-UV luminescence of FF nano- and microstructures were observed earlier and assigned either to n–π^* electronic transitions in the carbonyl group [6] or to the emission of exciton localized within the single nanotube (confined in about 9–10 Å) [17]. Furthermore, the photoluminescence (PL) was found to depend on the morphology of the tubes [10,18] and served as an indicator of the water presence [19]. Strong above-room temperature dependence of near-UV luminescence was observed by Gan et al. [20] rendering FF self-assembled structures as absolute temperature probes for bioapplications. However, the nature of the PL from FF structures is still elusive and current work is focused on studying their low-temperature emission. In this case, both exciton–phonon interactions and non-radiative recombination rates are reduced, which facilitates studying excitonic processes in bioinspired structures such as FF.

2. Materials and methods

The lyophilized form of the diphenylalanine (H–D–Phe–D–Phe–OH, FF) peptide was purchased from Bachem (Bubendorf, Switzerland). The solvent 1,1,1,3,3,3-hexafluoro-2-propanol (HFP) was purchased from Sigma-Aldrich. Fresh peptide stock solution was prepared by dissolving the peptide powder in HFP at a concentration of 100 mg/ml. To avoid any pre-aggregation, fresh stock solutions

* Corresponding author.
** Corresponding author at: Institute of Natural Sciences, Ural Federal University, Lenin ave. 51, 620000 Ekaterinburg, Russia.
E-mail addresses: kopel@ifi.unicamp.br (Y.V. Kopelevich), kholkin@gmail.com (A.L. Kholkin).

http://dx.doi.org/10.1016/j.physleta.2016.02.043
0375-9601/

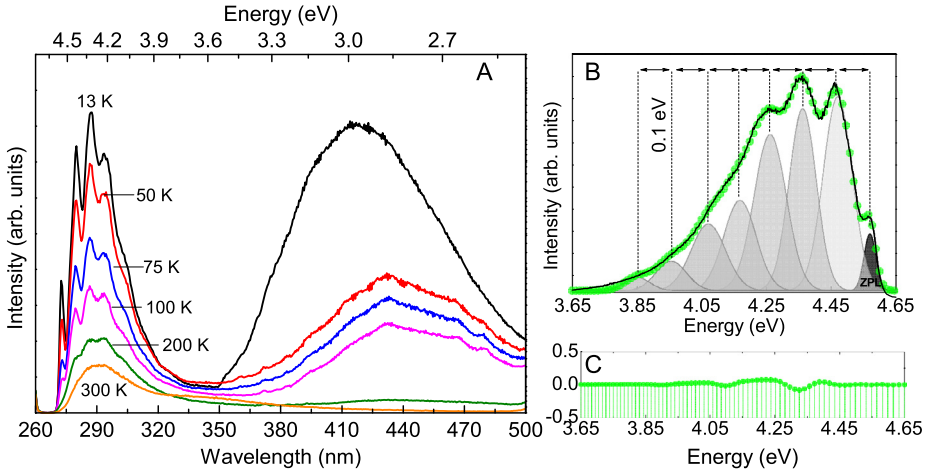

Fig. 1. (A) PL emission spectra of the FF microtubes excited at 255 nm for various temperatures. (B) PL emission spectrum (13 K) and the corresponding Gaussian components (shadowed areas) of the cumulative curve (circles). (C) Fit residual plot (coefficient of determination $r > 0.99$).

were prepared before each experiment. FF peptide stock solution was then diluted with distilled water (pH 6.67) to a final concentration of 2 mg/ml. Poly(tetrafluoroethylene) (PTFE) substrates were rinsed with ethanol and then with water in an ultrasonic bath for 10 min. In this work we have used the following method of sample preparation: first, 2 µL of FF stock solution was applied to the substrate and then 98 µL of water was added [1]. The resulting drops were dried at room temperature for one day. FF peptide tubes were then removed from the substrate and obtained powder of FF peptide tubes was stored at low temperature. Typical dimensions of the microtubes ranged from 1 to 5 µm in diameter and from 100 to 1000 µm in length. The microtubes consisted of multiple nanotubes as evidenced from the scanning electron microscopy (SEM) micrographs (see Fig. S1 of the Supplementary Information). SEM images also showed that a small fraction of the studied microtubes were in fact microrods (without a visible hole at the end). The structure of microtubes did not significantly change after repetitive cooling to liquid nitrogen temperature and below (Fig. S2).

The PL spectra were recorded in the temperature range from 320 to 12 K with a Horiba Scientific modular double grating excitation spectrofluorometer and a TRIAX 320 emission monochromator (Fluorolog-3) coupled to a R928 Hamamatsu photomultiplier by using the front-face acquisition mode. The excitation source was a 450 W Xe arc lamp. The temperature was controlled by a He closed-cycle cryostat and a Lakeshore 330 auto-tuning temperature controller with a resistance heater.

3. Results and discussion

Fig. 1 shows the typical emission spectra of peptide microtubes excited at 255 nm in near-UV and visible spectral ranges for various temperatures. At room temperature the emission spectra reveal a near-UV broad band centered at ~290 nm and a weaker shoulder at about 340 nm. Below 200 K, a series of narrower peaks in the near-UV band and a strong near-UV/blue/green emission (at 350–500 nm) appear. The near-UV band resembles that already reported by several authors [17,20], and will be the focus of this work as the visible luminescence at longer wavelengths is negligible at room temperature. We measured also the ratio Δ between the integrated intensity of these two emissions (at 290 and 350–500 nm, see Fig. S3A of the Supplementary Information) that can serve as a ratiometric thermometric parameter at low temperatures. We calculated the relative temperature sensitivity [21] defined as $S_r = \frac{\partial \Delta}{\partial T}/\Delta$ in the temperature range from 13 to 200 K (Fig. S3B of the Supplementary Information). Three distinct temperature regions of the S_r vs. T behavior are clearly identified: i) 13–60 K, where S_r decreases from 3.44 to 0.03% $\cdot$ K^{-1}; ii) 60–100 K, where S_r is maximum around 85 K (0.31% $\cdot$ K^{-1}), and iii) 100–200 K, where S_r gradually increases up to 1.97% $\cdot$ K^{-1}.

Gan et al. reported a thermometric behavior in FF nanotubes at high temperature (278–338 K) through the temperature dependence of the intensity of the UV broad band and its lifetime [20]. We notice that the ratiometric (or self-referencing) readout based on the intensity ratio is indeed required for this purpose. Using the luminescence intensity ratio for temperature sensing is much more reliable because it is not compromised by the well-known experimental errors arising from the critical dependence of the PL intensity on the sensor concentration, material inhomogeneities, and optoelectronic drifts of the excitation source and detectors [21].

The low-temperature emission spectrum in the near-UV region was fitted by a sum of the Gaussian bands, revealing that they all are energetically equidistant (by ~0.1 eV), which could correspond to the energy of the phonons replicated the main narrow peak at 4.54 eV (zero phonon line, ZPL in Fig. 1B).

In order to estimate the fundamental absorption edge and the forbidden energy bandgap (E_g) of the studied FF microtubes we measured the diffuse reflectance (R) as a function of the energy of the incident UV radiation. For monodisperse and thick samples with size comparable to the wavelength of the incident light, E_g can be estimated through the equation $R \propto (h\upsilon - E_g)^{n/2}$, where n is equal to 1 or 3 for direct and indirect bandgap semiconductors, respectively [22]. E_g was calculated using the linearization of the previous equation, $R^2 \propto (h\upsilon - E_g)$ for direct band gap semiconductors [23]. The diffuse reflectance data was fitted in the linear region by a straight line. Extrapolation of this line to zero reflectance yielded the value of the forbidden bandgap $E_g = 4.69 \pm 0.03$ eV at room temperature (Fig. 2A). It is thus can be inferred that FF microtubes can be described as a direct bandgap semiconductor that emits in the UV spectral region via annihilation of the excitons after illumination by the near-bandgap radiation.

Fig. 2B represents the temperature dependence of the photoluminescence excitation (PLE) spectra of the peptide microtubes obtained by monitoring the emission maximum at 305 nm. The room-temperature excitation spectrum shows a broad band with an absorption edge around 269 nm (4.6 ± 0.2 eV), resembling that found in the emission spectrum. Similarly to the behavior of the PL emission, the intensity of the excitation spectra increases with decreasing temperature. For temperatures below 200 K, the PLE spectra consist of multiple narrower peaks (Fig. 2C). We notice that all the peaks are again energetically equidistant (~0.1 eV) as observed for the emission spectra. Amdursky et al. reported a similar

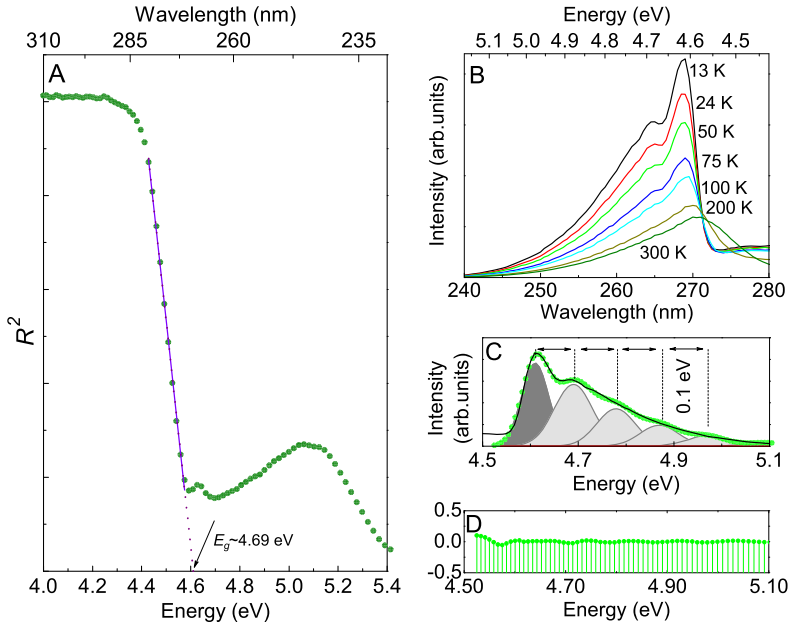

Fig. 2. (A) Reflectance squared (R^2) as a function of the energy of incident UV radiation of the FF microtubes; the solid line corresponds to the data best fit, $r > 0.99$. (B) PLE spectra as a function of the temperature monitored at 305 nm and (C) the corresponding Gaussian components (shadowed areas) of the cumulative curve (circles) at 13 K. (D) Fit residual plot ($r > 0.99$).

PLE spectrum for peptide nanospheres (synthesized with smaller concentration of FF monomers) at room temperature [24]. They associated the peak with the highest intensity at ~265 nm with the formation of excitons, whereas the appearance of multiple peaks in the excitation spectra was explained by the interaction of excited electrons with lattice vibrations. The difference in the energetic positions of excitation and emission spectra are naturally explained by the Stokes shift (about 0.3 eV at room temperature).

The exciton binding energy E_x is determined by the difference between the bandgap energy ($E_g = 4.69 \pm 0.03$ eV, Fig. 2A) and the position of the broad emission peak ($E_b \approx 4.35$ eV, Fig. 1A):

$$E_x = E_g - E_b. \tag{1}$$

The obtained value of the exciton binding energy $E_x \approx 0.34$ eV is smaller than that derived by Amdursky et al. (Ref. [27]) and it is intermediate between Frenkel and Wannier–Mott cases [25,26]. In a typical organic material with low dielectric constant, binding energy is a few eV and exciton is localized due to the strong Coulomb interaction. In a homogeneous semiconductor with high dielectric constant the exciton binding energy is a few tens of millielectronvolts [25]. We assume that it is the quantum confinement that determines sufficiently high binding energy of excitons in peptide microtubes. However, the lower value of the binding energy as compared to that determined in Ref. [26] is a signature of the less localized behavior. This also explains why the maximum of emission is shifted to lower energies in our case.

Amdursky et al. [27] derived the following equation for the size of the exciton localized in the quantum dot:

$$R = \pi r_B^0 \sqrt{\frac{m_{0/M}}{\frac{\mu}{\epsilon_\infty^2 m_0} - \frac{E_x}{Ry}}}, \tag{2}$$

where $r_B^0 = \hbar^2/m_0 e^2 = 0.53$ Å is the Bohr radius of the hydrogen atom, m_0 is the free electron mass, $Ry = m_0 e^4/2\hbar^2 = 13.56$ eV is the Rydberg constant, $M = m_e + m_h$ is the translation mass of the exciton (m_e and m_h are the effective electron and hole masses, respectively), $\mu = m_e m_h/(m_e + m_h)$ is the reduced exciton mass, and ε_∞ is the high-frequency dielectric constant.

Using the same parameters as in Ref. [27], except for the dielectric constant $\varepsilon_\infty = 3$ that was directly measured for pressed peptide powder, we obtained the localization length R of about 38 Å. This value is higher than that reported by Amdursky et al. [27] and can be related to defects in the microtube structure or the size of nanotube clusters rather than to the individual wall thickness.

In order to get further insight into the excitonic processes in peptide microtubes, we plotted the ZPL intensity (the high-energy peak in Fig. 1A) as a function of temperature. This dependence is depicted in Fig. 3A. When there is a non-radiative channel of recombination, the rate equation governing the density of the photogenerated excitons can be written as

$$\frac{\partial n}{\partial t} = G - \frac{n}{\tau_R} - \frac{n}{\tau_{NR}}, \tag{3}$$

where n is the density of the photogenerated excitons, G is the generation rate, and τ_R and τ_{NR} are radiative and nonradiative lifetimes, respectively [28]. Non-radiative rate is typically thermally activated (due to level depopulation or due to activation of non-radiative center), i.e. $\tau_{NR} = \tau_0 \exp(\frac{E_a}{k_B T})$. Steady-state luminescence intensity is proportional to n/τ_R, i.e. the following equation describes thermal quenching of the excitonic luminescence:

$$I(T) = \frac{I_0}{1 + Ae^{(-E_a/k_B T)}}, \tag{4}$$

where I_0 is the intensity at $T = 0$ K, $A = \tau_R/\tau_0$ and E_a is the activation energy of thermal quenching [28,29]. Fitting of experimental results shows that a single activation energy is sufficient to describe the temperature dependence of the ZPL emission in FF microtubes (Fig. 3A). The best fit is obtained for the thermal quenching energy $E_a = 0.021 \pm 0.002$ eV, which is about an order of magnitude lower than the obtained exciton binding energy ($E_x \sim 0.34$ eV). It should be stressed that the apparent thermal energy is generally lower than the optical one due to the existence of excited states or crystal field that can be split by spin–orbital interaction [28]. We hypothesize that the excitons can be stabilized in shallow radiative traps with the energy difference E_a. These

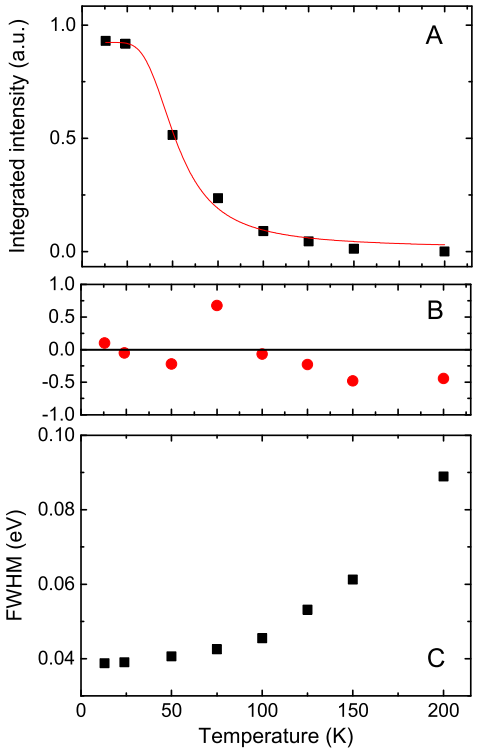

Fig. 3. (A) Temperature dependence of the normalized integrated intensity of the zero-phonon emission line at 4.54 eV (13 K). The solid line represents the best-fit curve obtained using Eq. (4). (B) Regular residual plot (coefficient of determination $r > 0.99$). (C) FWHM of temperature dependence of zero-phonon luminescence line.

radiative centers can be, for example, the intrinsic structural defects in peptide microtubes. Deng et al. [30] recently simulated such defects, which could form due to the mismatch between layer stacking along the side-chain direction and peptide growth along the H-bond direction. The higher the temperature, the closer thermal energy kT (~17 meV at 200 K) becomes to the energy of the excitons localized at these defects E_a (~21 meV). This in turn increases the probability of the excitons to leave the localized radiative state and recombine non-radiatively at other structural or an impurity related defects dissipating their energies to phonons. Thermal dependence of the full-width-at-half-maximum (FWHM) of the ZPL (Fig. 3C) shows a gradual broadening of the ZPL peak with increasing temperature due to interaction of excitons and acoustic phonons, which is fully consistent with the intensity variation (Fig. 3A).

FF nanotubes represent a unique class of self-assembled materials with the individual tube diameters of about 1.8 nm [31]. Correspondingly, a deep Frenkel-type exciton state appears due to localization effect at the distance of the order of 1 nm (distance between two adjacent channels in the nanoporous structure) [31]. This corresponds to the narrow blue luminescence peak observed by Amdursky et al. [17]. For the microtube arrangement, strong hydrogen bonds and hydrophobic interactions keep the entire structure in a crystalline form [32]. The exciton energy levels are therefore more shallow and thermal quenching leads to a strong decrease of the PL intensity with increasing temperature.

Recently observed optical wavequiding effect (Refs. [32,33]) in the microtubes evidences high optical quality of self-assembled FF microtubes and their usefulness for interfacing [34] with living cells or other biosystems. The observed strong temperature variation of the ratio between the near-UV and visible PL emission can be used for thermography at low temperatures thus complementing the high temperature study (Ref. [20]). In comparison with Ref. [20], our study reports a self-reference microthermometry based on the intensity ratio of two luminescent bands of FF peptides. Sufficiently high relative sensitivity (comparable e.g. to that of metal organic framework nanostructures) [35] makes it promising for cryobiology.

4. Conclusions

To summarize, the photoluminescent properties of diphenylalanine microtubes were studied in the temperature range from 12 to 300 K. Two bands have been identified: near-UV emission centered at 290 nm and visible emission at 350–500 nm. The UV luminescence decreases with the increasing temperature and exhibits several equidistant lines associated with zero-phonon exciton emission line and its phonon replicas. The PL quenching is connected with thermally activated exciton traps (with the activation energy of about 20 meV) such as defects in the crystalline structure of FF microtubes. FF microtubes are identified as direct optical bandgap material with the bandgap of ~4.69 eV at room temperature. The possibility of using them as an absolute temperature probe at low temperature is discussed.

Acknowledgements

The research was made possible by Russian Scientific Foundation (Grant 14-12-00812). The authors wish to thank Alexandre Botas, and Profs. Rute Ferreira and Luis Carlos for the help with photoluminescence measurements and fruitful discussions. Part of this work was developed in the scope of the project CICECO – Aveiro Institute of Materials (Ref. FCT UID/CTM/50011/2013), financed by national funds through the FCT/MEC and, when applicable, co-financed by FEDER under the PT2020 Partnership Agreement.

Appendix A. Supplementary material

Supplementary material related to this article can be found online at http://dx.doi.org/10.1016/j.physleta.2016.02.043.

References

[1] K. Ariga, T. Mori, J.P. Hill, Adv. Mater. 24 (2012) 158.
[2] C. Valery, F. Artzner, M. Paternostre, Soft Matter 7 (2011) 9583.
[3] L. Adler-Abramovich, E. Gazit, Chem. Soc. Rev. 43 (2014) 6881.
[4] Y.L. Yang, U. Khoe, X.M. Wang, A. Horii, H. Yokoi, S.G. Zhang, Nano Today 4 (2009) 193.
[5] M. Yemini, M. Reches, J. Rishpon, E. Gazit, Nano Lett. 5 (2005) 183.
[6] J. Ryu, S.Y. Lim, C.B. Park, Adv. Mater. 21 (2009) 1577.
[7] T. Cipriano, G. Knotts, A. Laudari, R.C. Bianchi, W.A. Alves, S. Guha, ACS Appl. Mater. Interfaces 6 (2014) 21408.
[8] M. Reches, E. Gazit, Science 300 (2003) 625.
[9] M. Reches, E. Gazit, Nano Lett. 4 (2004) 581.
[10] Q. Li, Y. Jia, L. Dai, Y. Yang, J. Li, ACS Nano 3 (2015) 2689.
[11] J. Kim, T.H. Han, Y.L. Kim, S. Park, J. Choi, D.G. Churchill, S.O. Kim, H. Ihee, Adv. Mater. 22 (2010) 583.
[12] L. Adler-Abramovich, N. Kol, I. Yanai, D. Barlam, R.Z. Shneck, E. Gazit, I. Rousso, Angew. Chem. Int. Ed. 49 (2010) 9939.
[13] M. Wang, L. Du, X. Wu, S. Xiong, P.K. Chu, ACS Nano 5 (2010) 4448.
[14] A.L. Kholkin, N. Amdursky, I. Bdikin, G. Rosenman, E. Gazit, ACS Nano 4 (2010) 610.
[15] J. Ryu, S.Y. Lim, C.B. Park, Adv. Mater. 21 (2009) 1577.
[16] R. De La Rica, H. Matsui, Chem. Soc. Rev. 39 (2010) 3499.
[17] N. Amdursky, M. Molotskii, D. Aronov, L. Adler-Abramovich, E. Gazit, G. Rosenman, Nano Lett. 9 (2009) 3111.
[18] X. Yan, J. Li, H. Moehwald, Adv. Mater. 23 (2011) 2796.
[19] M. Wang, S. Xiong, X. Wu, P.K. Chu, Small 7 (2011) 2801.
[20] Z. Gan, X. Wu, J. Zhang, X. Zhu, P.K. Chu, Biomacromolecules 14 (2012) 2112.
[21] C.D.S. Brites, P.P. Lima, N.J.O. Silva, A. Millan, V.S. Amaral, F. Palacio, L.D. Carlos, Nanoscale 4 (2012) 4799.
[22] B. Karvaly, I. Hevesi, Z. Naturforsch. A 26 (1971) 245.

[23] B. Akdim, R. Pachter, R.R. Naik, Appl. Phys. Lett. 106 (2015) 183707.
[24] N. Amdursky, M. Molotskii, E. Gazit, G. Rosenman, Appl. Phys. Lett. 94 (2009) 261907.
[25] I. Pelant, J. Valenta, Luminescence Spectroscopy of Semiconductors, Oxford University Press, 2012.
[26] V.M. Agranovich, Excitations in Organic Solids, Oxford University Press, 2008.
[27] N. Amdursky, M. Molotskii, E. Gazit, G. Rosenman, J. Am. Chem. Soc. 132 (2010) 15632.
[28] T. Makino, K. Tamura, C.H. Chia, Y. Segawa, M. Kawasaki, A. Ohtomo, H. Koinuma, J. Appl. Phys. 93 (2003) 5929.
[29] M. Leroux, N. Grandjean, B. Beaumont, G. Nataf, F. Semond, J. Massies, P. Gibart, J. Appl. Phys. 86 (1999) 3721.
[30] Li Deng, Yurong Zhao, Hai Xu, Yanting Wang, Appl. Phys. Lett. 107 (2015) 043701.
[31] C.H. Gorbitz, Chem. Commun. 2332 (2006).
[32] X. Yan, J. Li, H. Moehwald, Adv. Mater. 23 (2011) 2796.
[33] A. Handelman, B. Apter, N. Turko, G. Rosenman, Acta Biomater. (2015), http://dx.doi.org/10.1016/j.actbio.2015.11.004.
[34] S. Hoffmann, H. Hagenmuller, A.M. Koch, R. Muller, C. Vunjak-Novakovic, D.L. Kaplan, H.P. Merkle, L. Meinel, Biomaterials 28 (2007) 115.
[35] A. Cadiau, C.D.S. Brites, P.M.F.J. Costa, R.A.S. Ferreira, J. Rocha, L.D. Carlos, ACS Nano 7 (2013) 7213.